Med Biol Eng Comput (2006) 44: 131–139
DOI 10.1007/s11517-005-0006-0

ORIGINAL ARTICLE

Eddie Y. K. Ng · W. Kee Ng

Parametric study of the biopotential equation for breast tumour identification using ANOVA and Taguchi method

Received: 9 August 2005 / Accepted: 25 October 2005 / Published online: 26 January 2006

Abstract Extensive literatures have shown significant trend of progressive electrical changes according to the proliferative characteristics of breast epithelial cells. Physiologists also further postulated that malignant transformation resulted from sustained depolarization and a failure of the cell to repolarize after cell division, making the area where cancer develops relatively depolarized when compared to their non-dividing or resting counterparts. In this paper, we present a new approach, the Biofield Diagnostic System (BDS), which might have the potential to augment the process of diagnosing breast cancer. This technique was based on the efficacy of analysing skin surface electrical potentials for the differential diagnosis of breast abnormalities. We developed a female breast model, which was close to the actual, by considering the breast as a hemisphere in supine condition with various layers of unequal thickness. Isotropic homogeneous conductivity was assigned to each of these compartments and the volume conductor problem was solved using finite element method to determine the potential distribution developed due to a dipole source. Furthermore, four important parameters were identified and analysis of variance (ANOVA, Yates' method) was performed using 2^n design (n = number of parameters, 4). The effect and importance of these parameters were analysed. The Taguchi method was further used to optimise the parameters in order to ensure that the signal from the tumour is maximum as compared to the noise from other factors. The Taguchi method used proved that probes' source strength, tumour size and location of tumours have great effect on the surface potential field. For best results on the breast surface, while having the biggest possible tumour size, low amplitudes of current should be applied nearest to the breast surface.

E. Y. K. Ng (✉) · W. K. Ng
School of Mechanical and Aerospace Engineering,
College of Engineering, Nanyang Technological University,
50, Nanyang Avenue, 639798 Singapore, Singapore
E-mail: mykng@ntu.edu.sg

Keywords Biofield Diagnostic System · Parametric optimisation · ANOVA · Breast tumour · Taguchi · Yates

1 Introduction

Breast cancer continues to be the most frequent type of cancer diagnosed among women in Singapore. Last year alone, more than 1,000 cases were detected (3 per day) and breast cancer kills 5 women there every week. It is known that the early detection of tumour ensures better prognosis and higher survival rate. The existing Biofield Diagnostic System (BDS—intelligent diagnostic tool) is to be studied in detail for breast cancer detection, which is inexpensive and non-invasive. This tool will be based on biopotential measurement made from electrodes on breast surface in conjunction with numerical simulation of the breast using the biopotential equation. The basic idea lies in the notion that tissues differ in their dielectric properties. Potential distribution between the preliminarily classified abnormal breast is then mapped with a controlled probe placed on the palm of the patient. BDS injects small electrical currents through arrays of probes placed on the surface of a patient body and measures the voltages needed to maintain these currents. Then the inverse problem (though not so straightforward) is to be solved to approximate the electrical conductivity changes inside the solution domain given the applied currents and equipotential lines on the surface. Once the conductivity is known, the underlying material could be predicted, in particular the possible presence of water as in water cysts or mineral deposits. Initial clinical trials [2] suggested that the test can achieve a sensitivity of approximately 90% and a specificity of 40–50%, which indicates that the test might be useful for excluding cancer when it is, in fact, absent. Therefore, we believe that the BDS, in complement to other existing techniques such as mammography, ultrasound or MRI, can make a clinically significant and cost-effective adjunct procedure for the early detection of breast cancer. Of

course, it is to be noted that the ultimate diagnosis of the disease still lies in the results from fine needle biopsy.

In this paper, we present a geometrically realistic breast model with common breast dimensions and the theoretical sampling set-up of BDS device to examine its validity in the detection and diagnosis of malignant breast lesions and also parametric optimisation of the mode. The underlying mechanism that governs the physiological basis of the idea that tissue differentiation may plausibly be based on measurements of the dielectric properties has been presented in our earlier publications [12, 13]. A spherical disturbance due to the tumour is artificially included in an excited domain. The strength of the electric field is controlled using the excitation current injected through the surface probes. A method of data analysis and parametric optimization for the model will be introduced.

2 Methods

2.1 The Biofield Diagnostic System

In the present interest on BDS examination[1] [2], a direct current electric field is applied between the patient palm and both breasts surfaces non-invasively. The BDS consists of the Biofield Diagnostic Device (hereafter referred to as the Device) and Biofield Diagnostic Sensors (hereafter referred to as the Sensors). The Device is a desktop-sized electronic device, enclosed in a plastic case, with software, keyboard, liquid crystal display, printer and patient cable. The single-use sensors are pregelled with a specifically formulated electro-conductive medium. No energy or radiation is introduced into the body. The examination, which takes approximately 20 min, is conducted by placing single-use sensors on the breast and subxiphoid, recording DC electropotentials and then analysing these potentials [2]. The output of a test is immediately available and provides an objective index of breast malignancy in the area examined, based on comparing cellular proliferation in the breast tissue. The diagnostic test, in order to be conducted, requires a suspicious lesion to be located by either palpation or other procedures and so is an adjunctive diagnostic test, by design. The measuring probe, which contains a standard array of eight sensors per breast, is localized as shown (Fig. 1). The initial clinical diagnostic studies conducted in Europe and USA indicated that breast cancers produced significantly greater electropotential differentials between the normal breast as compared to the lesions [2, 16, 21]. With these encouraging results and with the superior BDS now available in the market, it was decided to revisit this field in collaboration with the Singapore General Hospital. In order to build confidence in the numerical modelling, an extensive theoretical work was undertaken. As a first step, two- and three-dimensional models, which were a close representative of the actual shape, were developed. Direct numerical simulation was done and results analysed for breast with tumours of various sizes at different locations. However, it is also to be noted that each parameter, such as probe source strength and tumour conductivity, has a different degree of influence towards the end results. In this paper, we conduct an analysis of variance (ANOVA) to better explain the precedence and the importance of the various factors. Once this is identified it would help in classifying the factors as noise or nuisance factors. If these factors can be controlled then it would help in setting up a protocol and in identifying the factor of interest, that is, the existence of tumour.

[1]There is another commercial product that uses a similar arrangement of electrodes and compares the load impedances bilaterally (Z-tech, Inc. [22]) for breast cancer screening, particularly some of the instrumentation developments. There are also groups working with planar arrays of electrodes instruments, some of which are currently undergoing clinical trials (T-scan [20], for example).

2.2 Numerical modelling

Most bioelectric applications involve signals of sufficiently low frequency such that the displacement current, which is governed by the permittivity of tissue, is much smaller than the conduction current. The distribution of electrical potential ϕ within an inhomogeneous anisotropic conducting medium can be expressed by the quasi-static Poisson equation:

$$\nabla \cdot (\sigma \nabla \phi) = I_{\mathrm{V}}, \tag{1}$$

where ϕ is the electric potential, σ the tissue space variant conductivity tensor and I_{v} any source term existing in the solution domain. For well-posed problems having a single solution, we solved the governing equation by using the conventional methods of Weighted Average Residual Theorem. We then developed a female breast model, which is close enough to the actual. Ng and Sudharsan [11] considered the breast as a hemisphere in supine condition with various layers of unequal thickness, based on a cross-sectional view of the anatomy of female breast as presented in Romrell and Brand [15]. We assumed the breast to be of hemispherical shape with a 5 mm subcutaneous layer, followed by a gland and muscle layer of varying thickness. The three-dimensional model is presented as in Fig. 2 [12], based on the breast mammogram from Yale Medical School [19]. For the dimension of the breast, we considered a diameter of 144 mm and a height of 70 mm, where these parameters more closely mimic the average size of an Asian woman breast in supine condition. Figure 3 shows a typical breast examination performed with the BDS [2]. Note that the nipple is not modelled at this stage for numerical simulation due to its complexity in surface potential.

This geometrical model is considered to be more accurate for the following assumptions and parameters:

1. The actually varying thicknesses of the breast layers were also taken into consideration.

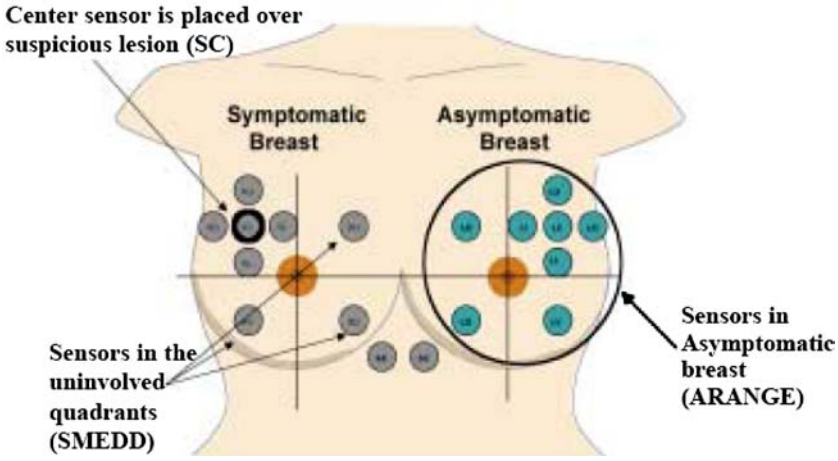

Fig. 1 Sensor placement for suspicious lesion in right upper outer quadrant [2]

2. The curves representing each layers and boundaries were drawn using a polynomial equation of second order (though it is an approximation to build a numerical model of a breast).

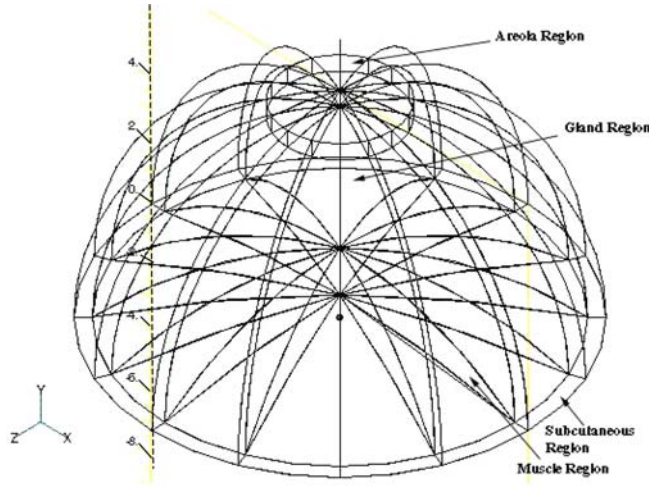

(a) A typical schematic view of 3D model

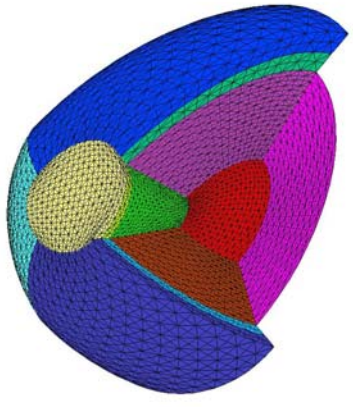

(b) Mesh used in the 3D model

Fig. 2 Computational model of breast comprising various layers [12]

3. A patient was assumed to be in supine position (lying down flat). Therefore, it is acceptable to assume the model to be near hemispherical. Further complexities in geometry will be considered as part of future works.
4. Room temperature was assumed to be the same as the temperature of the skin surface. Studies of the treatment of the room temperature effect in the overall bioelectric field in the solution domain were not considered in the present analysis.
5. The surface of the breast was assumed to have no electrical conduction with the ambient. Hence, the Neumann condition was appropriate.

Assuming an inhomogeneous domain but constant homogeneous conductivity (σ) for each layer, the potential distribution is computed by solving Poisson equation with known imposed currents applied at appropriate surface node locations. The air in contact with the body has negligible conductivity, and the ratio of body conductivity to air conductivity is infinite. The electrical conduction system in each layer of the breast is taken to be isotropic, although in reality, there exists variation in conductivities depending on the direction, since the muscle fibres and subunits are not aligned in parallel. Additional complexities arise because the breast wall is not just muscle but contains bone, adipose tissue and skin. Hence, at the surface of breast that is in contact with the ambient, the surface current inhomogeneous Neumann boundary condition of

$$(\sigma \nabla \phi).n = h \tag{2}$$

is specified. h describes the electrical current flux density ($\mathrm{mA/m^2}$) entering and leaving the breast over the dipoles, as excitation current. With this boundary condition and a homogeneous conductivity distribution estimated throughout each layer of tissues at the interior of the breast, the potential distribution can be solved using numerical approach, in particular the finite element method (FEM) in the present effort. Once ϕ is known at each node point, electrical intensity E can be computed using negative gradient of potential:

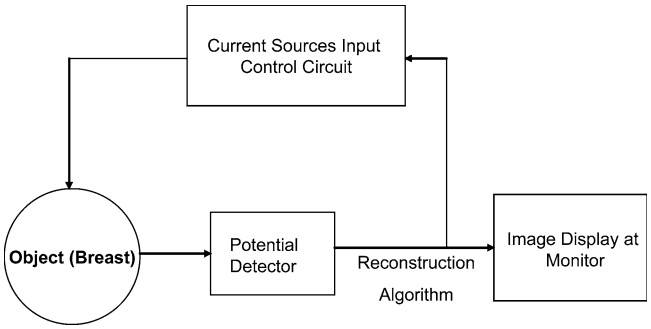

Fig. 3 A block diagram for the BDS [2]

$$E = -\nabla\phi. \tag{3}$$

In this model, the boundary in contact with the torso is tagged as zero. The reason is to prevent any potential field (noises) from interfering with the potential distribution of breast by the dipole and to confine all the excitation forces in the breast without passing to the torso.

3 Results

A Cartesian coordinate system was employed on the segmented breast model. Solution domain was discritized using quadratic Lagrange elements. In this model, there are 36,000 elements and it satisfies the mesh-independent solution [12] based on grid convergence index and Richardson error criterion [14]. Equation 1 was solved in FEMLAB [3] using the classical FEM. FEMLAB is a high-level PDE calculator and stands for Finite Element Modelling Laboratory. It is an advanced software package for modelling and simulation of any physical process one can describe with partial differential equations. FEMLAB has built-in high-performance state-of-the-art solvers that address extremely large problems, yet quickly yield accurate results. The in-house highly efficient GMRES[2] solver was used in the computational domain. For this linear solver we provided a relative tolerance of 1.0×10^{-3} for the linear iterations and unlimited number of iterations for the solver to achieve convergence. We also set a factor of 40 in the error estimate, which acts as a safety factor. Finally, we set the restart value of 50 to specify the number of iterations the solver performs until it restarts. This larger value we select can lead to high accuracy in the iterative process but with an increase in memory use.

For the convergence criterion of the total residual that we initially set to 10×10^{-3}, the iterative algorithm, the sensitivity matrix calculated may contain large errors at the area of interest. We designed the meshing of the domain such that denser mesh was applied at the area at which we predict a steep electric potential gradient. The simulation was carried out on a Pentium IV PC, consuming 6–7 min of the net CPU time per run.

[2]An iterative linear algorithm for unsymmetric problems.

Table 1 High and low properties values used for the various breast numerical models

Factor	Description	Low	High	Units
A	Probes' source strength	1	10	mA
B	Tumour size (diameter)	5	17	mm
C	Tumour conductivity	850	1,236	S/m
D	Location of tumour	70.0	0.0	degrees

3.1 Analysis of variance (Yates' method)

It was decided to analyse the factors that affect the breast surface potential difference and their order of importance. We consider a three-dimensional model of the breast with tumour within the fats region, which is the outermost layer. The factors considered are probes' source strength (the magnitude of the applied currents), tumour size, tumour conductivity and tumour location along the fats region. A 2^n factorial design was used where each factor would have two levels of low and high values with a total of 16 runs.

The source strength of the four probes is set at 1 mA for low value and 10 mA for high value. The tumour sizes are 5 mm (low) and 17 mm (high) in diameter. The tumour conductivity is fixed at 850 S/m (low) and 1,236 S/m (high).[3] The low and high values are summarised in Table 1. For low tumour, location is at 70° ($R = 62$ mm) away from the y-axis along the subcutaneous layer. Its high location is at the tip of the breast (0°, $R = 62$ mm) in the centre of the y-axis, as denoted in Figs. 4 and 5. The factors are denoted in upper case and the runs (parameters combination of Table 2) in lower case by convention.

The runs conducted are as: (1), a, b, c, d, ab, ac, ad, bc, bd, cd, abc, abd, acd, bcd, abcd. Run (1) corresponds to simulation conducted where all the factors are at low level. A presence of a lower case letter in the run signifies that the simulation is conducted by fixing the value corresponding to that factor (denoted in upper case) at the high level and the rest at low level. Such combination of high and low levels would yield a total of 16 runs for 4 factors.

The observation is taken at the breast surface. The ANOVA results are tabulated in Table 2 using Yates' method [10]. We used pooling and pooled all sum of square (SS) of third and higher order interactions (abc, abd, acd, bcd, abcd) to provide estimation of error variance. SS in the table denotes sum of square which is given by $g^2/n = g^2/16$, n being the number of data points; DOF is the degree of freedom; mean square, which is given by SS/DOF, is also equal to the estimates of variance effect; error of the method is defined by

[3]Once tumour grows in size, there is a possibility of necrosis and this might alter the tumour conductivity. This is because the metabolic rate and tumour doubling time changes. However, it takes years for a tumour to grow for older subjects in particular (it behaves as a progressive and heterogeneous disease), and the earliest possible indication of abnormality is needed to allow for the earliest possible treatment and intervention.

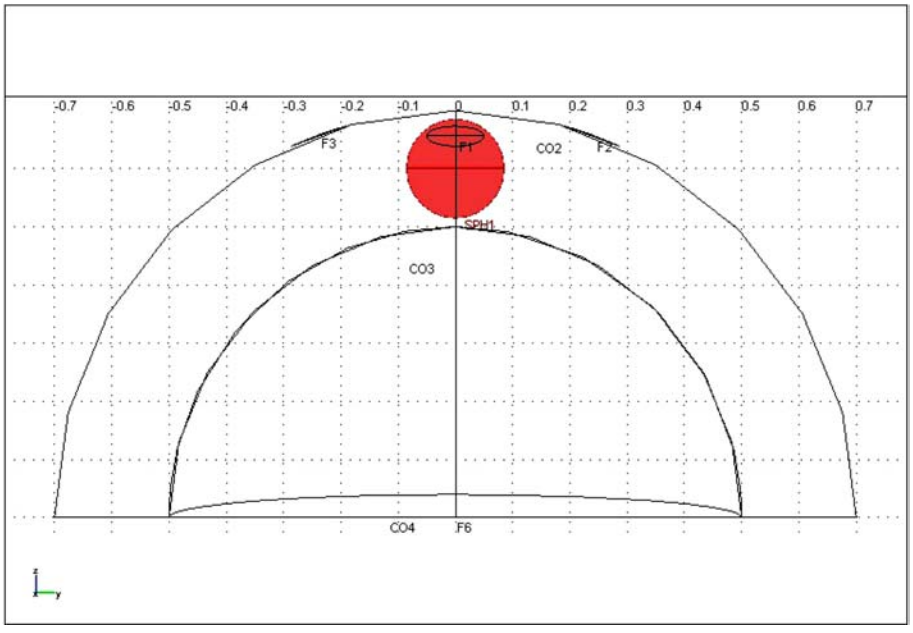

Fig. 4 High tumour location ($\theta = 0°$, $R = 62$ mm)

variance error, which is given by ($g_{abc} + g_{abd} + - g_{acd} + g_{bcd} + g_{abcd}$)/5; and finally F, the variance effect divided by variance error, gives SS/error. From the F-table at 5% level of significance, we tabulated that $F_{0.05;\,1,\,16} = 4.49$. As shown in the above Yates' table, factors A, B and D are greater than 4.49 and thus have significant effect on the surface potential field.

3.2 Taguchi method

Taguchi separates factors into two main groups: control factors and noise factors. Noise factors are those over which we have no direct control but which vary with the breast environment [18]. The control factors that may contribute to reduced variation (improved quality) can be quickly identified by looking at the amount of variation present as a response. It is our aim to be able to capture the signal from the tumour (i.e. a global view of the potential distribution on the breast surface, as computed and expressed as values at all the surface nodes) rather than that from those three more significant factors (A, B and D). We apply an analysis based on the Taguchi method [18] widely used in quality engineering to build in robustness in the experimental set-up.

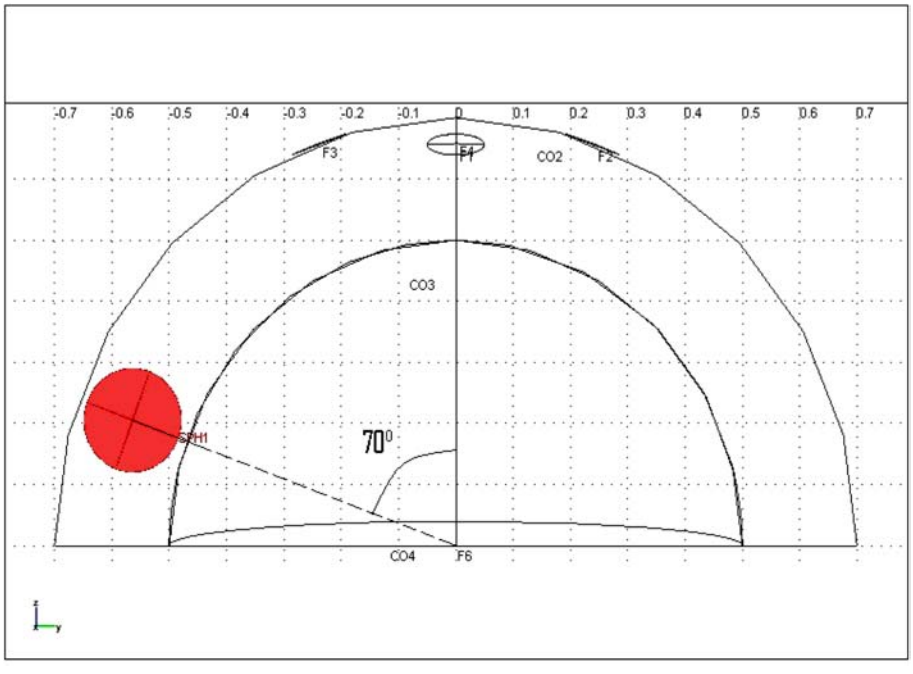

Fig. 5 Low tumour location ($\theta = 70°$, $R = 62$ mm)

Table 2 Analysis of Yates' method

1Parameters combination	2Response (yield)	3	4	5	6*g*	SS	DOF	Mean square	*F*
(1)	7.25839×10^{-4}	4.35832×10^{-3}	8.72186×10^{-3}	1.74260×10^{-2}	3.37887×10^{-2}	–	–	–	–
a	3.63248×10^{-3}	4.36354×10^{-3}	8.70414×10^{-3}	1.63627×10^{-2}	2.25277×10^{-2}	3.17185×10^{-5}	1	3.17185×10^{-5}	14,021.931
b	7.26257×10^{-4}	4.33976×10^{-3}	8.20085×10^{-3}	1.16221×10^{-2}	-5.60173×10^{-4}	1.96121×10^{-8}	1	1.96121×10^{-8}	8.670
ab	3.63728×10^{-3}	4.36438×10^{-3}	8.16183×10^{-3}	1.09056×10^{-2}	-3.77359×10^{-4}	8.89997×10^{-9}	1	8.89997×10^{-9}	3.934
c	7.23545×10^{-4}	4.25143×10^{-3}	5.81767×10^{-3}	2.98384×10^{-5}	-5.67353×10^{-5}	2.01181×10^{-10}	1	2.01181×10^{-10}	0.089
ac	3.61622×10^{-3}	3.94942×10^{-3}	5.80440×10^{-3}	-5.9001×10^{-4}	-3.79369×10^{-5}	8.99505×10^{-11}	1	8.99505×10^{-11}	0.040
bc	7.26324×10^{-4}	4.22492×10^{-3}	5.46514×10^{-3}	2.34460×10^{-5}	3.34093×10^{-5}	6.97611×10^{-11}	1	6.97611×10^{-11}	0.031
abc	3.63806×10^{-3}	3.93692×10^{-3}	5.44046×10^{-3}	-4.0080×10^{-4}	2.85740×10^{-5}	5.10298×10^{-11}	1	–	–
d	7.07594×10^{-4}	2.90664×10^{-3}	5.21823×10^{-6}	-1.7714×10^{-5}	-1.06331×10^{-3}	7.06645×10^{-8}	1	7.06645×10^{-8}	31.239
ad	3.54384×10^{-3}	2.91102×10^{-3}	2.46202×10^{-5}	-3.9021×10^{-5}	-7.16471×10^{-4}	3.20832×10^{-8}	1	3.20832×10^{-8}	14.183
bd	6.60264×10^{-4}	2.89267×10^{-3}	-3.02010×10^{-4}	-1.32617×10^{-5}	-6.1985×10^{-4}	2.40134×10^{-8}	1	2.40134×10^{-8}	10.616
abd	3.28916×10^{-3}	2.91173×10^{-3}	-2.88002×10^{-4}	-2.4675×10^{-5}	-4.2425×10^{-4}	1.12493×10^{-8}	1	–	–
cd	7.03980×10^{-4}	2.83624×10^{-3}	4.38287×10^{-6}	1.94020×10^{-5}	-2.1306×10^{-5}	2.83714×10^{-11}	1	2.83714×10^{-11}	0.013
acd	3.52094×10^{-3}	2.62889×10^{-3}	1.90631×10^{-5}	1.4007×10^{-5}	-1.1413×10^{-5}	8.14163×10^{-12}	1	–	–
bcd	6.56706×10^{-4}	2.81696×10^{-3}	-2.07349×10^{-4}	1.46802×10^{-5}	-5.3947×10^{-6}	1.81892×10^{-12}	1	–	–
abcd	3.28021×10^{-3}	2.62350×10^{-3}	-1.93455×10^{-4}	1.38938×10^{-5}	-7.86453×10^{-7}	3.86568×10^{-14}	1	–	–
Error							5	2.26206×10^{-9}	
Total SS	3.37887×10^{-2} 1.03240×10^{-4}								

where SS = sum of square = $g^2/n = g^2/16$; n = number of data points; DOF = f = degree of freedom; mean square = SS/DOF = estimates of variance effect; error = variance error = $(g_{abc} + g_{abd} + g_{acd} + g_{bcd} + g_{abcd})/5$; F = variance effect/variance error = SS/(DOF×error)

Table 3 Analysis using Taguchi method

		A (LOW)		A (HIGH)		T_{avg}	Total variation, S_t	Average variation, S_m	Error variation, S_e	Error variance, V_e	S/N
		B (LOW)	B (HIGH)	B (LOW)	B (HIGH)						
C (LOW)	D (LOW)	7.27217×10^{-4}	7.26257×10^{-4}	7.25211×10^{-3}	7.24799×10^{-3}	3.98839×10^{-3}	1.0618275×10^{-4}	6.3629131×10^{-5}	4.255621×10^{-5}	1.4184540×10^{-5}	−0.5976
	D (HIGH)	7.25691×10^{-4}	6.60264×10^{-4}	7.24510×10^{-3}	6.60854×10^{-3}	3.80990×10^{-3}	9.7126851×10^{-5}	5.8061314×10^{-5}	3.9065537×10^{-5}	1.3021846×10^{-5}	−0.6314
C (HIGH)	D (LOW)	7.27217×10^{-4}	7.26324×10^{-4}	7.25156×10^{-3}	7.30446×10^{-3}	4.00239×10^{-3}	1.0699665×10^{-4}	6.4076511×10^{-5}	4.2920139×10^{-5}	1.4306713×10^{-5}	−0.6063
	D (HIGH)	7.25640×10^{-4}	6.56706×10^{-4}	7.24393×10^{-3}	6.60829×10^{-3}	3.80864×10^{-3}	9.7101835×10^{-5}	5.8023000×10^{-5}	3.9078834×10^{-5}	1.3026278×10^{-5}	−0.6370
T_{avg}		7.26441×10^{-4}	6.92388×10^{-4}	7.24818×10^{-3}	6.94232×10^{-3}						
Total variation, S_t		2.1108700×10^{-6}	1.9222071×10^{-6}	2.1014422×10^{-4}	1.9323079×10^{-4}						
Average variation, S_m		2.1108676×10^{-6}	1.9176032×10^{-6}	2.1014416×10^{-4}	1.9278323×10^{-4}						
Error variation, S_e		2.4084527×10^{-12}	4.6039178×10^{-9}	5.4418100×10^{-11}	4.4756466×10^{-7}						
Error variance, V_e		8.0281758×10^{-13}	1.5346393×10^{-9}	1.8139367×10^{-11}	1.4918822×10^{-7}						
S/N (dB)		58.1778	24.9434	64.6184	25.0894						

In the Taguchi method, quality is measured by the deviation of a characteristic from its target value. A loss function is developed for this deviation. Uncontrollable factors, known as noise, cause such deviation and thereby lead to loss. Since elimination of noise factors is impractical and often impossible, the Taguchi method seeks to minimise the effect of noise and to determine the optimal level of the important controllable factors based on the concept of robustness. In this method, the controllable factor is separated from the uncontrollable factors and the analysis is carried out to find the best setting for the controllable factors that would yield the optimum result irrespective of the variation in magnitude of the uncontrollable factor. Taguchi has created a transformation of the repetition data to another value which is a measure of the variation present. The transformation is the signal-to-noise (S/N) ratio. The S/N ratio consolidates several repetitions (at least two data points are needed) into one value that reflects the amount of variation present.

The aim is to maximise the signal (i.e. surface potential from the tumour size and location) to the noise (i.e. associated from tumour conductivity). Table 3 summarizes the surface potential field predicted with respect to the interaction of the parameters A, B, C and D. We are using the non-dynamic output response application: nominal best method to get the Taguchi table above. It is seen that a non-dynamic approach is useful for a specific test with a fixed output.

The nominal best S/N ratio is described as

$$S/N = \text{desired output/undesired output} = \text{effect of the average/variability around the average.}$$

Calculations for a nominal best S/N ratio are as follows. There are n pieces of data:

$$y_1,\ y_2,\ y_3, \ldots\ldots, y_n \quad (\text{DOF} = f = n).$$

The total variation S_t is

$$S_t = y_1^2 + y_2^2 + y_3^2 + \cdots + y_n^2.$$

The average variation S_m is

$$S_m = (y_1 + y_2 + y_3 + \cdots + y_n)^2/n \quad (f = 1).$$

The error variation S_e is

$$S_e = S_t - S_m \quad (f = n - 1).$$

The error variance V_e is the error variation divided by its degree of freedom (DOF):

$$V_e = S_e/(n-1).$$

The S/N ratio is given by

$$S/N = \frac{10\log(1/n)(S_m - V_e)}{V_e}.$$

For an example, to calculate the S/N value of interaction between parameters A (low), B (low), we have

four data values 7.27217×10^{-4}, 7.25691×10^{-4}, 7.27217×10^{-4}, 7.25640×10^{-4}:

$$S_t = (7.27217 \times 10^{-4})^2 + (7.25691 \times 10^{-4})^2 + (7.27217 \times 10^{-4})^2 + (7.25640 \times 10^{-4})^2 = 2.1108700 \times 10^{-6}.$$

$$S_m = (7.27217 \times 10^{-4} + 7.25691 \times 10^{-4} + 7.27217 \times 10^{-4} + 7.25640 \times 10^{-4})^2/4 = 2.1108676 \times 10^{-6}.$$

$$S_e = S_t - S_m = 2.1108700 \times 10^{-6} - 2.1108676 \times 10^{-6} = 2.4084527 \times 10^{-12}.$$

$$V_e = S_e/(n-1) = 2.4084527 \times 10^{-12}/(4-1) = 8.0281758 \times 10^{-13}.$$

$$S/N = \frac{10\log(1/n)\ (S_m - V_e)}{V_e} = 58.1778.$$

Table 4 summarizes the effect and the signal-to-noise for various factors. The effect is computed by taking the mean T_{avg}, which represents a particular condition. For example, effect of Factor A at low level is computed by taking the two T_{avg} corresponding to A at low level and divided by 2:

$$\text{A (LOW)} = (7.26441 \times 10^{-4} + 6.92388 \times 10^{-4})/2 = 0.0007094.$$

Similarly,

$$\text{C (HIGH)} = (0.004002 + 0.003809)/2 = 0.0039055.$$

4 Discussion

4.1 Comparison with literature

Long before the discovery of any screening tool, Fricke and Morse [4] have found that, in comparison with benign tumours or with inactive tissues of the same or similar characters, certain types of malignant tumours are associated with rather high capacity and significantly higher permittivity of breast tumour tissues in vitro at 20 kHz. Furthermore, those most important type malignant tumours have high capacity as compared with benign tumours of a similar character and also with the normal tissue in which they lie. The characterization of the biophysical features of cancerous breast tissue has captured the great interest of researchers, both from a screening and therapeutic point of view. Many analytical and critical reviews of the literatures on dielectric properties of breast tissues at radiowave and microwave frequencies are presented. The frequencies of measurements are reviewed objectively, and the frequency used in the current study is justified.

Table 4 Effect and S/N ratio for various factors used

Factor		Low	High
Probes' source strength A	Effect	0.0007094	0.0070952
	S/N	41.5606435	44.8538685
Tumour size B	Effect	0.0039873	0.0038174
	S/N	61.3980957	25.0164163
Tumour conductivity C	Effect	0.0038991	0.0039055
	S/N	−0.6144788	−0.6216672
Location of tumour D	Effect	0.0039954	0.0038093
	S/N	−0.6019523	−0.6341937

Some useful works were documented by Chaudhary et al. [1]. Chaudhary et al. measured the dielectric constant of malignant tissues at frequencies below 100 MHz and threw some light on the future electromagnetically based (EM) techniques for cancer treatment and detection tools. They observed that the relative dielectric constant of malignant tissue was strikingly higher than that of the normal tissue, particularly at frequencies below 100 MHz. The relative permittivities of normal and malignant tissues at frequencies below a few megahertz would be wider. This encourages researchers in EM radiation scanning technique to develop or refine their equipments for detection of an early stage of breast cancer.

Similar reliable finding was reported by Surowiec et al. [17]. Surowiec et al. worked on the relative permittivity of infiltrating centre part of breast carcinoma, tumour-surrounding tissue and the peripheral tissue. Their experiments were performed at frequencies from 20 kHz to 100 MHz at 37°C using an automatic network analyser and an end of the line capacitive sensor. The results also seem to indicate modality for the detection of human breast carcinoma.

Joines et al. [6] measured the electrical conductivity and relative permittivity of malignant and normal tissues from various tissue origins including mammary gland. Joines et al. concluded that at all frequencies tested, both parameters showed greater magnitude in malignant tissue than in normal tissue of the same type, especially in tissues from the mammary gland.

Jossinet and Schnitt [7] studied the definition and evaluation of dielectric properties in the characterization and differentiation of freshly excised breast tissues. Their work was mainly within the frequency range of 0.488 kHz to 1 MHz. They showed significant differences between most of the breast tissue groups, especially between cancerous tissue and all the other tissue groups. This further confirmed that electrical properties of the tissues can be considered as potentially suitable for the distinguishability of the presence of malignancy in breast tissues.

Among the studies, the works of Surowiec et al. [17] and Jossinet and Schnitt [7] appear to be most reliable and relevant to our analysis. Studies were done on the centre and surrounding breast tissues of tumour at normal body temperature. This enhances the general knowledge and understanding of the natural proliferating tumour. The measurement frequencies of both

literatures are from 20 kHz to 100 MHz. However, Morimoto et al. [9] argued that this did not imply that at lower frequency, biopotential analysis could not provide adequate variation in dielectric parameters for potential diagnostic purpose. In fact, based on in vivo measurement of electrical properties up to 200 kHz, elements of the Fricke [4] equivalent circuit model for breast tumours differed significantly from those for benign tumours.

4.2 Strength and limitations of the methods

Signal-to-noise ratio (S/N or SNR) is a measure of signal strength relative to background noise [5] and is calculated above using Taguchi method. The tabulated results show that in order to receive the effect of tumour conductivity on the breast surface, factors A, B and D have great influences on the effect.

Both Yates' and Taguchi methods used proved that probes' source strength, tumour size and location of tumours have great effect on the surface potential field. For best results on the breast surface, the probes strength should be low while having the tumour size and location high. While tumour with higher conductivity would have better detection on the breast surface, however, this also means that it would produce slightly higher background noise. A future work would be to maximize the signal difference between a normal breast model and one with a tumour (i.e. for cases of bilateral abnormalities).

Finally, while DC measurements may be sufficient to identify a malignant lesion, it is generally thought among researchers in the field that the reactance, the complex part of the impedance, holds more information that is useful in differentiating normal or benign tissues from malignant ones [8].

5 Conclusion

The ANOVA results using Yates' method shows that the probes' source strength A, tumour size B and location of the tumour D have significant effect on the breast surface electropotentials.

Acknowledgements The authors would like to express their appreciation to Dr. J. Cuzick of Biofield Corp., Alpharetta, USA, for sharing his views and interests on "The breast cancer diagnostic system".

References

1. Chaudhary SS, Mishra RK, Swarup A, Thomas JM (1984) Dielectric properties of normal and malignant human breast tissues at radiowave and microwave frequencies. Indian J Biochem Biophys 21:76–79
2. Cuzick J, Holland R, Barth V, Davies R, Faupel M, Fentiman I, Frischbier HJ, LaMarque JL, Merson M, Sacchini V, Vanel D, Veronesi U (1998) Electropotential measurements as a new diagnostic modality for breast cancer. Lancet 352:359–363
3. FEMLAB Software. http://www.comsol.com/products/femlab/ (assessed 26 July 2005)
4. Fricke H, Morse S (1926) The Electric capacity of tumors of the breast. J Cancer Res 16:310–376
5. Huigen E, Peper A, Grimbergen CA (2002) Investigation into the origin of the noise of surface electrodes. Biol Eng Comput 40(3):332–338
6. Joines WT, Zhang Y, Li C, Jirtle RL (1994) The measured electrical properties of normal and malignant human from 50 to 900 MHz. Med Phys 21:547–550
7. Jossinet J, Schnitt M (1999) A review of parameters for the bioelectrical characterization of breast tissue. Ann NY Acad Sci 873:30–34
8. Modre R, Tilg B, Fischer G, Hanser F, Messnarz B, Seger M, Hintringer F, Roithinger FX (2004) Ventricular surface activation time imaging from electrocardiogram mapping data. Med Biol Eng Comput 42(2):146–150
9. Morimoto T, Kimura S, Konishi Y, Komaki K, Uyama T, Monden Y, Kinouchi Y, Iritani T (1993) A study of the electrical bio-impedance of tumors. J Invest Surg 6:25–32
10. Natrella MG (1996) Experimental statistics. Revised edition Wiley, New York
11. Ng EYK, Sudharsan NM (2001) An improved 3-D direct numerical modeling and thermal analysis of a female breast with tumour. Int J Eng Med Proc IME Part H 215(1):25–37
12. Ng WK, Ng EYK, Ang WT, Lim J (2004) Simulation of biofield potential for early detection of breast tumor with a realistic female model and artificially inserted carcinoma. In: Proceedings of the international conference on biomedical engineering, Kuala Lumpur, Malaysia, 2–4 September 2004, pp 229–232
13. Ng EYK, Ng WK, Ang WT, Sim LSJ, Rajendra Acharya U (2005) Modelling of biofield potential for early detection of breast tumor with FEM. Comput Methods Programs Biomed (in press)
14. Roache PJ (1994) Perspective: a method for uniform reporting of grid refinement studies. ASME J Fluids Eng 116:405–413
15. Romrell LJ, Bland KI (1991) Anatomy of breast, axilla, chest wall, and related metastatic sites. In: Bland KI, Copeland EM III (eds) The breast: a comprehensive management of benign and malignant diseases. Saunders, Philadelphia, p 22
16. Sacchini V (1996) Report of the European School of Oncology Task Force on electropotentials in the clinical assessment of neoplasia. Breast 5:282–286
17. Surowiec AJ, Stuchly SS, Barr JR, Swarup A (1988) Dielectric properties of breast carcinoma and the surrounding tissues. IEEE Trans Biomed Eng 35:257–263
18. Taguchi G (1986) Introduction to quality engineering. Asian Productivity Organization/UNIPUB, White Plains
19. The Yale Medical School. http://www.info.med.yale.edu/intmed/cardio/imaging/anatomy/breast_anatomy/ (assessed 26 July 2005)
20. T-scan Breast Imaging. http://www.imaginis.com/t-scan/ (assessed 26 September 2005)
21. Weiss BA, Ganepola GAP, Freeman HP, Hsu YS, Faupel ML (1994) Surface electric potentials as a new modality in the diagnosis of breast lesions—a preliminary report. Breast Dis 7:91–98
22. Z-Tech, Inc. http://www.z-techinc.com/how.html (assessed 26 September 2005)